Agronomy Research **15**(S1), 971–980, 2017

Wear and stress analysis of chisel

R. Chotěborský[1,*], M. Linda[2] and M. Hromasová[2]

[1]Czech University of Life Sciences, Faculty of Engineering, Department of Material Science and Manufacturing, Kamycka 129, CZ165 21 Prague, Czech Republic
[2]Czech University of Life Sciences, Faculty of Engineering, Department of Electrical Engineering and Automation, Kamycka 129, CZ165 21 Prague, Czech Republic
[*]Correspondence: choteborsky@tf.czu.cz

Abstract. The object of research is stress analysis of worn chisel. The interaction between soil particles and chisel leads to change of shape and dimension of a worn chisel or other agriculture tools. The wear rate depends on the velocity of the chisel in the soil, position in the soil and shape of a chisel. These factors change the dimension and shape of chisel during its service life. The modern chisel includes sintered carbides on a tip. Sintered carbides plates are effective protection for wear resistance. But the body of the chisel is not protected and its wear resistance is lower than the tip. The service life of the tip is much higher than the body of the chisel. Stresses of the body of the chisel are stationary during the service life. The aim of this study is determining of optimising process of the strength of steel for chisels.

Key words: agriculture tools, FEM, soil, wear.

INTRODUCTION

Agriculture tools like chisel are most used for a non-tillage agriculture operation. Soil as particular media content a different ratio of particle size, usually sand particles and other, and its mineral composition depend on the place of land. A lot of researchers have been described a mineralogical composition (Singh et al., 2015), particular composition (De Pellegrin & Stachowiak, 2001), moisture content and other chemical and physical properties of soil (Rajaram & Erbach, 1998; Mouazen, 2002; Vogel et al., 2005; Asaf et al., 2007; Tagar et al., 2014). Some researchers have been focused on rheological properties of the soil and they have been described mechanical properties of soil for a prediction its behaviour under loading, wetting and drying (Rajaram & Erbach, 1998; Coetzee & Els, 2009; Tang et al., 2011; Chen et al., 2013; Sima, Jiang, & Zhou, 2014). Mathematical models of soil we can develop by finite element methods, discrete element methods or boundary element methods. Mechanical properties of soil are mostly described by finite element method, ex. under press loading. But drying of soil has been described by discrete element methods or more complicated by finite element methods. The interaction between soil and agriculture tools can be developed by a complex method where the first solver solve flow of soil around the tools, ex. Discrete element method and second solver transform force and velocity to the stress-strain analysis of tools, ex. Finite or discrete element method (Araya & Gao, 1995; Mouazen & Neményi, 1999; Mouazen & Ramon, 2002; Karmakar et al., 2007; Maksarov & Olt, 2008; Rojek

et al., 2011; Guo et al., 2012; Mak et al., 2012; Bentaher et al., 2013; Jørgensen, 2014; van Wyk et al., 2014; Farid Eltom et al., 2015; Borys & Küüt, 2016; Zhu et al., 2016). Although stress analysis in finite element method can be solved by steady state, the flow of soil is transient solver in discrete element method. Also present model of interaction between soil and agriculture tools used a modern mathematical methods (Abu-Hamdeh, 2003; Abo-Elnor et al., 2004; Aluko & Chandler, 2004), but the solution has unexpected change of shape during soil processing, thanks to wearing process in soil (Stachowiak, 2000; Stachowiak & Stachowiak, 2001; Waoldman et al., 2012; Woldman et al., 2015). A complex model of interaction can be generalized with heat treatment of steel and input to the mathematical model, it can be wide for optimizing the process for manufactory production, where we can solve interaction of soil with tools and their heat treatment for the best service life and fuel consumption.

Some study showed that the microstructure, mechanical properties and wear can be predicted by mathematical models (Natsis et al., 2008).

The aim of this study is to present an idea of optimising process for a chisel, its heat treatment and stress analysis for best service life.

MATERIALS AND METHODS

The process of heat transfer during quenching of a steel chisel (Fig. 1) is nonstationary due to the variation of temperature with time. In this work, the problem of heat transfer, austenite phase transformation, flow, stress analysis in a three-dimensional phase was examined.

Figure 1. Real chisel computerization.

The structure composition of steel cooling depends on the actual hardness defined as:

$$HV = V_P \times HV_P + V_B \times HV_B + V_M \times HV_M \quad (1)$$

Where V_P is the volume of pearlite, V_B is the volume of bainite and V_M is the volume of martensite.

The amount of phases proportion is an equal unity defined by (Li et al., 2001; Liu et al., 2003; Pietrzyk & Kuziak, 2011; Xie et al., 2013) as:

$$HV_M = 127 + 949 \times C + 27 \times Si + 8 \times Ni + 16 \times Cr + 21 \times lnV_r \quad (2)$$

$$HV_B = -323 + 185 \times C + 330 \times Si + 153 \times Mn + 65 \times Ni + 144 \times Cr + 191 \times Mo + (89 + 53 \times C - 55 \times Si - 22 \times Mn - 10 \times Ni - 20 \times Cr - 33 \times Mo) \times lnV_r \quad (3)$$

$$HV_{F,P} = 42 + 233 \times C + 53 \times Si + 30 \times Mn + 12.6 \times Ni + 7 \times Cr + 19 \times Mo + (10 - 19 \times Si + 4 \times Ni + 8 \times Cr + 130 \times V) \times lnV_r \quad (4)$$

Where *C*, *Si*, *Mn* and others represent different kinds of chemical elements respectively (wt. %), V_r represents cooling speed at 700 °C (°C h^{-1}). The material was steel 25CrMo4 and heat treatment quenching in water.

From Eq. 1, it is not difficult to predict the fraction of phases if the hardness of cooling microstructure and the hardness of microstructure constituents' are separately known (Eqs 2 to 4). Results of austenite decomposition depend on the chemical composition and steel history. The characteristic cooling time relevant for structure transformation for most steel is the time $t_{8\text{-}5}$, this time is determined from temperature 800 °C to 500 °C. The characteristic cooling time was determined through series of algorithm where an average value of heat gradient between 500 °C and 800 °C.

The calculation of hardness was done by retrieving the temperature of nodes file. The analysis was performed for N nodes corresponding to the mesh of model. The temperature parameters of the nodes of the model were introduced (inlet) into the calculation of the volumetric representation of ferrite, pearlite, bainite and martensite.

The abrasive wear rate was determined according to ASTM G65 (ASTM G65-04, 2010). Samples were loaded by force 17 N, 35 N, 57 N, 78 N a 100 N in testing schema 3–1–3–1–3 (three times at 17 N, ones at 35 N, three times at 57 N). Repeated testing were used for elimination of testing errors according to DoE methods. The signification of slope the results of cumulative wear at same loading were tested on statistical dependency. The total track was 1890 m for one sample, the part track was 210 m. The mass loss was determined after part track on digital balance with accuracy 0.1 mg. The volume loss or wear was recalculated from mass loss divided by the density of steel 7,800 kg m^{-3}. The hardness of abrasive was Ha = 1,100 HV30.

Discrete element method was used for determination of flow soil particles around the chisel. Soil DEM model was determined from an experimental data of soil (sandy-loam) from land (GPS 50°23'36.2"N 16°01'47.2"E), where we done a practical tests. Experimental evaluation included pressing, relaxation, creep in pressing vessel and also included a shear test of soil at different loading. The output data included poison ratio, the coefficient of friction soil particle between itself, the dependency between young modulus and strain. These data were input for a DEM model of soil. Step size was 1 km. Results of DEM model (force and velocity) were applied on boundary nodes of surface chisel mesh model. The algorithm is schematically presented in Fig. 2.

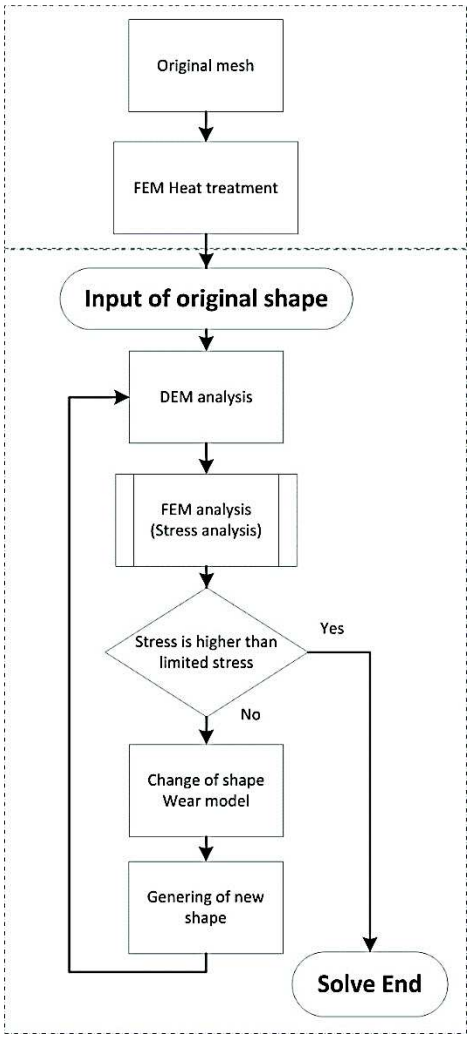

Figure 2. Schema of the algorithm.

Intel Xeon CPU E5-2640 v3 @ 2.60 GHz, 128 GB DDR3 RAM was used for an algorithm which was written in SciLab 5.5.2 (Scilab Enterprises, 2016).

RESULTS AND DISCUSSION

According to the schema of the algorithm (Fig. 2), the first step was determining of chisel microstructure and calculation of hardness. The result of quenched steel in cross section is presented in Fig. 3. FEM model showed that the microstructure and hardness were not homogenous although steel content hard martensitic structure and bainite after quenching. So, each of node in mesh model content a different ration two phases and according to Eq. 1 we determined hardness in this position of the node. This procedure we applied for all nodes in the model (Chotěborský & Linda, 2015). After then we

applied a model of wear rate. The original shape of the chisel was solved in DEM solver (Fig. 4) and results of particle flow (force and velocity) were applied in FEM model.

Figure 3. Hardness in cross section (near the hole in Fig. 4) of chisel after heat treatment.

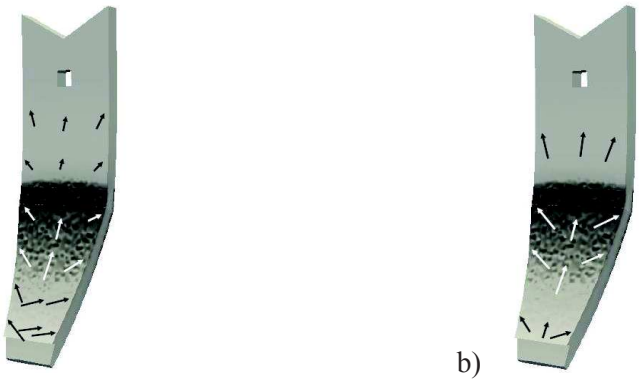

Figure 4. Vectors of force (a) and velocity (b) from DEM.

The mathematical model of wear W ($\mathrm{mm^3\ m^{-1}}$) was determined by using of general linear method with step by step solver in Statistica software. Mathematical models with and without interaction of variables were compared between themselves. Comparison criteria were quality of fitting (R), residua normality and half normality, F and p value for a models with and without intercept. The best model no include interception but with interaction of variables in factorial schema.

General mathematical model (5–8):

$$W = A \times \frac{F}{S} + B \times \frac{Ha}{Hm} + C \times \frac{F \times Ha}{S \times Hm} \tag{5}$$

where:

$$A = 9 \times 10^{-5} \pm 2 \times 10^{-5} \tag{6}$$

$$B = 1.03 \times 10^{-3} \pm 0.057 \times 10^{-3} \tag{7}$$

$$C = 7 \times 10^{-5} \pm 1 \times 10^{-5} \tag{8}$$

Total quality of model:

$R = 0.96; F = 6043; p \ll 0.001$

The limited factors:

$Ha \in \{600; 1100\}; Hm \in \{200; 800\}$ Vickers hardness at load 30 kg HV30, Ha–abrasive hardness, Hm–material–steel hardness calculated from Eq. 1 and *S* is area.

$F \in \{10; 100\}\, N; S = 2.64\ cm^2$

Full mathematical model for a simulation:

$$W = 9 \times 10^{-5} \times \frac{F}{S} + 1.03 \times 10^{-3} \times \frac{Ha}{Hm} + 7 \times 10^{-5} \times \frac{F \times Ha}{S \times Hm} \qquad (9)$$

Where the ratio of force F and area A can be changed by stress in kPa for a simulation. Although these model no include other variables like sharpness according to (Stachowiak, 1998; Stachowiak, 2000; Stachowiak & Stachowiak, 2001), we can use it as a simple for a next modelling. The results of DEM simulation of soil flow (force and velocity) are transformed to an algorithm for an each node on the surface boundary. Boundary nodes moving depend on results according to Eq. 9 and after then the mesh generator design a new mesh (Fig. 5). This algorithm continuously calculates stress analysis in FEM for a new mesh dimension.

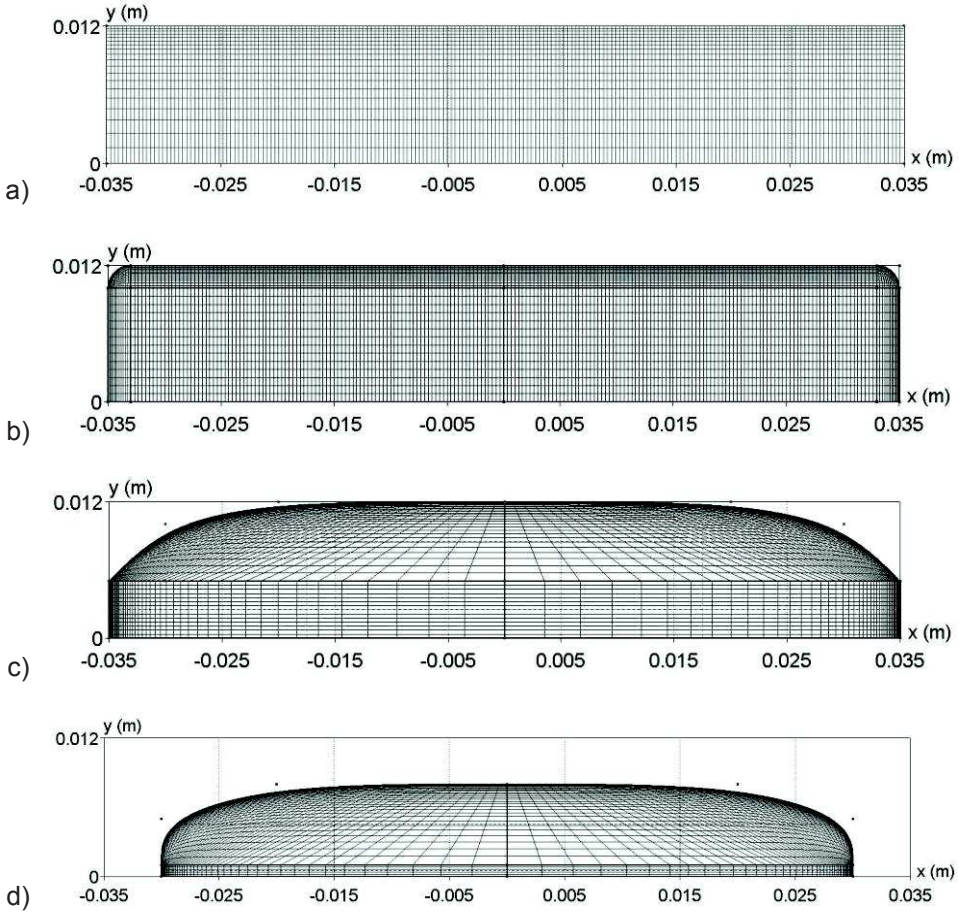

Figure 5. Cross section area of chisel mesh model; a) new chisel; b) 1 km distance; c) 5 km distance; d) 15 km distance.

Full new chisel model and worn chisel are presented in Fig. 7.

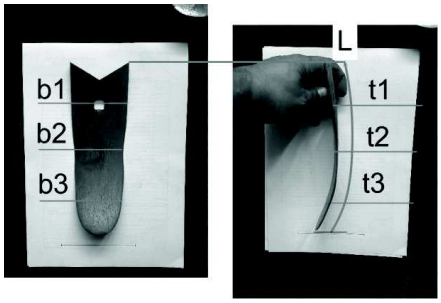

Figure 6. Real worn chisel after 15 km distance.

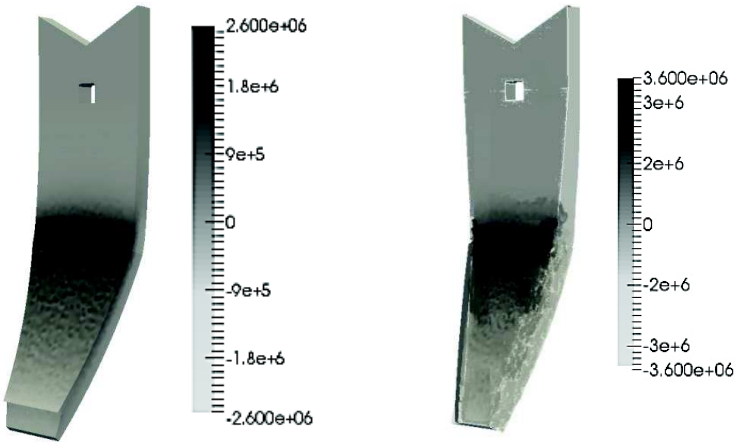

Figure 7. 3D Model of stress fields a new and worn chisel after 5 km.

Modelled and experimental measured data of thickness and width of chisel are presented in Fig. 8. The data showed good a correlation between modelled and measured the shape of chisel but residua are higher than 10%. Residues can be caused by larger abrasive particles of soil in the testing field, which were carried out practical field tests. Although the model showed similar soil moisture content. It can be caused by the mineral composition of soil, and that the soil contained a larger volume alumina silicates (Chotěborský & Linda, 2016), which are harder than sand and there are also sharper (Singh et al., 2006). Nevertheless, it is possible above procedure successfully applied for an overview of changes in shape during no-tillage. It is also possible to predict the traction resistance with the change of shape. However, our goal was to developed algorithms involving complex calculation chisel from the design of heat treatment to wear with an estimated stress in chisel, which leads to rupture or plastic deformation of the chisel during no-tillage agriculture operations. Especially, when the tip of chisel is protected by WC–Co sintered carbide with high wear resistance properties. This procedure is time-consuming for processor time, however, in our opinion is more accurate than the mathematical model based on experimental description change of

shape of chisel or ploughshare, for example as shown example GLM model (Arvidsson et al., 2004) or description of neural networks.

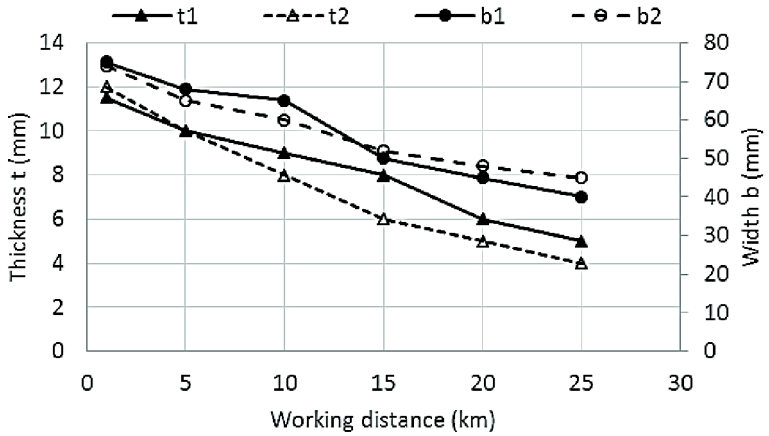

Figure 8. Thickness and width of the chisel, where t1 – measured thickness, t1 – modelled thickness, b1 – measured width (means) and b2 – modelled width.

CONCLUSIONS

The results presented in this article can be summarized in the following conclusions:

The algorithm is applicable for analysing stress of worn chisel. The results showed a good correlation between the measured data of shape changes in soil and modelled shape during wear.

The algorithm is time-consuming in case of one treated processing.

ACKNOWLEDGEMENTS. Supported by 31140/1414/314107 Technological agency of Czech Republic, 'R & D of working tools for agricultural machines'.

REFERENCES

Abo-Elnor, M., Hamilton, R. & Boyle, J. 2004. Simulation of soil–blade interaction for sandy soil using advanced 3D finite element analysis. *Soil and Tillage Research* **75**(1), 61–73.

Abu-Hamdeh, N. 2003. A nonlinear 3D finite element analysis of the soil forces acting on a disk plow. *Soil and Tillage Research* **74**(2), 115–124.

Aluko, O. B. & Chandler, H. W. 2004. Characterisation and Modelling of Brittle Fracture in Two-dimensional Soil Cutting. *Biosystems Engineering* **88**(3), 369–381.

Araya, K. & Gao, R. 1995. A Non-linear Three-Dimensional Finite Element Analysis of Subsoiler Cutting with Pressurized Air Injection. *Journal of Agricultural Engineering Research* **61**(2), 115–128.

Arvidsson, J., Keller, T. & Gustafsson, K. 2004. Specific draught for mouldboard plough, chisel plough and disc harrow at different water contents. *Soil and Tillage Research* **79**(2), 221–231.

Asaf, Z., Rubinstein, D. & Shmulevich, I. 2007. Determination of discrete element model parameters required for soil tillage. *Soil and Tillage Research* **92**(1–2), 227–242.

ASTM G65-04. Standard Test Method for Measuring Abrasion Using the Dry Sand/Rubber Wheel Apparatus (2010).
Bentaher, H., Ibrahmi, A., Hamza, E., Hbaieb, M., Kantchev, G., Maalej, A. & Arnold, W. 2013. *Finite element simulation of moldboard–soil interaction*. *Soil and Tillage Research* **134**.
Borys, N. & Küüt, A. 2016. The influence of basic soil tillage methods and weather conditions on the yield of spring barley in forest-steppe conditions. *Agronomy Research* **14**(2), 317–326.
Coetzee, C.J. & Els, D.N.J. 2009. Calibration of granular material parameters for DEM modelling and numerical verification by blade–granular material interaction. *Journal of Terramechanics* **46**(1), 15–26.
De Pellegrin, D. & Stachowiak, G.W. 2001. New technique for measuring particle angularity using cone fit analysis. *Wear* **247**(1), 109–119.
Farid Eltom, A.E., Ding, W., Ding, Q., Ali, A. baker B. & Eisa Adam, B. 2015. Effect of trash board on moldboard plough performance at low speed and under two straw conditions. *Journal of Terramechanics* **59**, 27–34.
Guo, L., Jirigalantu, & Zhang, F.C. 2012. The Load Analysis of Chisel-Edge Ruling Tool for Diffraction Gratings. *Applied Mechanics and Materials* **182–183**, 1596–1599.
Chen, Y., Munkholm, L.J. & Nyord, T. 2013. A discrete element model for soil–sweep interaction in three different soils. *Soil and Tillage Research* 126, 34–41.
Chotěborský, R. & Linda, M. 2015. FEM based numerical simulation for heat treatment of the agricultural tools. *Agronomy Research* **13**(3).
Chotěborský, R. & Linda, M. 2016. Determination of chemical content of soil particle for abrasive wear test. *Agronomy Research* **14**.
Jørgensen, M.H. 2014. Adaptive tillage systems. *Agronomy Research* 12(1), 95–100.
Karmakar, S., Kushwaha, R.L. & Laguë, C. 2007. Numerical modelling of soil stress and pressure distribution on a flat tillage tool using computational fluid dynamics. *Biosystems Engineering* **97**(3), 407–414.
Li, X., Miodownik, A.P. & Saunders, N. 2001. Simultaneous calculation of mechanical properties and phase equilibria. *Journal of Phase Equilibria* **22**(3), 247–253.
Liu, C.C., Xu, X.J. & Liu, Z. 2003. A FEM modeling of quenching and tempering and its application in industrial engineering. *Finite Elements in Analysis and Design* **39**(11), 1053–1070.
Mak, J., Chen, Y. & Sadek, M.A. 2012. Determining parameters of a discrete element model for soil–tool interaction. *Soil and Tillage Research* **118**, 117–122.
Maksarov, V. & Olt, J. 2008. Analysis of the rheological model of the process of chip formation with metal machining. *Agronomy Research* **6**, 249–253.
Mouazen, A. M. 2002. Mechanical behaviour of the upper layers of a sandy loam soil under shear loading. *Journal of Terramechanics* **39**(3), 115–126.
Mouazen, A.M. & Neményi, M. 1999. Finite element analysis of subsoiler cutting in non-homogeneous sandy loam soil. *Soil and Tillage Research* **51**(1), 1–15.
Mouazen, A.M. & Ramon, H. 2002. A numerical–statistical hybrid modelling scheme for evaluation of draught requirements of a subsoiler cutting a sandy loam soil, as affected by moisture content, bulk density and depth. *Soil and Tillage Research* **63**(3), 155–165.
Natsis, A., Petropoulos, G. & Pandazaras, C. 2008. Influence of local soil conditions on mouldboard ploughshare abrasive wear. *Tribology International* **41**(3), 151–157.
Pietrzyk, M. & Kuziak, R. 2011. Computer aided interpretation of results of the Jominy test. *Archives of Civil and Mechanical Engineering* **11**(3), 707–722.
Rajaram, G. & Erbach, D. 1998. Drying stress effect on mechanical behaviour of a clay-loam soil. *Soil and Tillage Research* **49**(1–2), 147–158.
Rojek, J., Oñate, E., Labra, C. & Kargl, H. 2011. Discrete element simulation of rock cutting. *International Journal of Rock Mechanics and Mining Sciences* **48**(6), 996–1010.

Scilab Enterprises. 2016. Scilab. France. *http://www.scilab.org/.* Accessed 21.11.2016
Sima, J., Jiang, M. & Zhou, C. 2014. Numerical simulation of desiccation cracking in a thin clay layer using 3D discrete element modeling. *Computers and Geotechnics* **56**, 168–180.
Singh, C.K., Kumar, P., Kumar, A. & Mukherjee, S. 2015. Depositional environment in great Indian desert using grain size parameters and its chemical characterization. *Journal of the Geological Society of India* **86**(4), 412–420.
Singh, M., Mondal, D.P. & Das, S. 2006. Abrasive wear response of aluminium alloy-sillimanite particle reinforced composite under low stress condition. *Materials Science and Engineering A* **419**(1–2), 59–68.
Stachowiak, G. & Stachowiak, G. 2001. The effects of particle characteristics on three-body abrasive wear. *Wear* **249**(3–4), 201–207.
Stachowiak, G.W. 1998. Numerical characterization of wear particles morphology and angularity of particles and surfaces. *Tribology International* **31**(1–3), 139–157.
Stachowiak, G.W. 2000. Particle angularity and its relationship to abrasive and erosive wear. In *Wear* **241**, 214–219.
Tagar, A.A., Ji, C., Ding, Q., Adamowski, J., Chandio, F.A. & Mari, I.A. 2014. Soil failure patterns and draft as influenced by consistency limits: An evaluation of the remolded soil cutting test. *Soil and Tillage Research* **137**, 58–66.
Tang, C.-S., Shi, B., Liu, C., Suo, W.-B. & Gao, L. 2011. Experimental characterization of shrinkage and desiccation cracking in thin clay layer. *Applied Clay Science* **52**(1–2), 69–77.
van Wyk, G., Els, D.N.J., Akdogan, G., Bradshaw, S.M. & Sacks, N. 2014. Discrete element simulation of tribological interactions in rock cutting. *International Journal of Rock Mechanics and Mining Sciences* **65**, 8–19.
Vogel, H.-J., Hoffmann, H. & Roth, K. 2005. Studies of crack dynamics in clay soil. *Geoderma* **125**(3–4), 203–211.
Woldman, M., Tinga, T., Van Der Heide, E. & Masen, M.A. 2015. Abrasive wear based predictive maintenance for systems operating in sandy conditions. *Wear* **338–339**, 316–324.
Woldman, M., van der Heide, E., Schipper, D.J., Tinga, T. & Masen, M.A. 2012. Investigating the influence of sand particle properties on abrasive wear behaviour. *Wear* **294–295**, 419–426.
Xie, J. Bin, Wu, C.C., Fan, J., Fu, M. & Hu, D.F. 2013. Numerical Simulation on the Temperature Field of Steel 1045 Quenched by Different Hardening Media. *Applied Mechanics and Materials* **444–445**, 1222–1228.
Zhu, L., Cheng, X., Peng, S.-S., Qi, Y.-Y., Zhang, W.-F., Jiang, R. & Yin, C.-L. 2016. Three dimensional computational fluid dynamic interaction between soil and plowbreast of horizontally reversal plow. *Computers and Electronics in Agriculture* **123**, 1–9.